International Astronomy and Astrophysics Research Journal

1(1): 67-76, 2019; Article no.IAARJ.53312

Theoretical Behaviour of $^{8}B + ^{208}pb$ Elastic Scattering within Double Folding Model

N. A. El-Nohy[1], M. N. El-Hammamy[2*], M. El-Azab Farid[3], A. Attia[1] and Moamen M. Elsayed[1]

[1]Department of Physics, Faculty of Science, Alexandria University, Alexandria, Egypt.
[2]Department of Physics, Faculty of Science, Damanhur University, Damanhur, Egypt.
[3]Department of Physics, Faculty of Science, Assiut University, Assiut, Egypt.

Authors' contributions

This work was carried out in collaboration among all authors. Authors NAEN and MNEH designed the study, performed the statistical analysis, wrote the protocol and wrote the first draft of the manuscript. Authors AA and MME managed the analyses of the study. Author MEAF managed the literature searches. All authors read and approved the final manuscript.

Article Information

Editor(s):
(1) Dr. Swarniv Chandra, Assistant Professor, Department of Physics, Techno India University, India.
(2) Dr. Magdy Rabie Soliman Sanad, Professor, Department of Astronomy, National Research Institute of Astronomy and Geophysics, Cairo, Egypt.
Reviewers:
(1) U. C. Srivastava, Amity University, India.
(2) Orchidea Maria Lecian, Comenius University, Bratislava, Slovakia.
(3) Branko Vuković, University of Osijek, Croatia.
Complete Peer review History: http://www.sdiarticle4.com/review-history/53312

Original Research Article

Received 18 October 2019
Accepted 23 December 2019
Published 10 January 2020

ABSTRACT

In this paper, we discuss the behavior of exotic nucleus ^{8}B elastic scattering from heavy target ^{208}pb at two different energies; 50 MeV (coulomb energy) and 170.3 MeV . For this purpose, we perform double folding (DF) calculations by treating ^{8}B as a ($^{7}Be+P$) and ($^{7}B+n$) core-nucleon system and evaluate the central part of the nuclear optical potential. The calculations including real and imaginary optical potentials are shown to reproduce very well the elastic scattering cross sections obtained by folding the density independent (DIM3Y) effective nucleon-nucleon interaction with the halo density distribution of the ^{8}B nucleus. The results of the two configurations similarly describe satisfactorily relevant experimental data. This confirms the validity of the halo structure of the ^{8}B nucleus within these models.

**Corresponding author: E-mail: marwa1374@yahoo.com;*

Keywords: Elastic scattering; double folding; halo nuclei.

PACS: 25.70.Bc, 24.10.Ht, 27.20.+n., 21.60.Gx.

1. INTRODUCTION

Recently, the short-lived radioactive nucleus ^{8}B with low breakup separation energy 0.1375 MeV, close by the proton drip line, has conveyed pretty much interest because of its significant role in the creation of high energy neutrinos in the sun and its quite unusual structure as one-proton halo nucleus [1]. Consequently, it is being a perfect contender for nuclear reaction mechanism examinations with exotic nuclei. Besides, the studies on ^{8}B reaction-mechanism processes are somewhat exiguous because of the difficulty of producing the ^{8}B beam produced only in a very few facilities and in all cases with low intensities [2-4]. Thus, the structure and reaction mechanism of ^{8}B have pulled in sharp consideration from both hypothetical and trial perspectives.

Numerous confirmations bolster a halo structure of ^{8}B. The measurements of interaction cross sections confirmed that the root mean square (rms) radius of ^{8}B is different in a comparison to more tightly bound Boron isotopes [5,6]. Just as, the relativistic mean field calculations [7] demonstrate that ^{8}B has a large proton matter radius put one next to the other to its neutron matter radius. Moreover, many other experimental results [8,9] are an indication of the large spatial extension of the loosely bound proton in ^{8}B.

It has been found that the elastic scattering, a simple process, is a valuable probe to contemplate the size and surface diffuseness of exotic nuclei by looking at likenesses and contrasts in reactions induced by weakly bound and tightly bound nuclei. Many intriguing phenomena have been discovered by examining the elastic scattering angular distributions for light neutron halo nuclei. A lot of elastic scattering experiments have been performed for neutron halo nuclei, such as ^{6}He [10-17] and ^{11}Be [18,19]. However, elastic scattering data for proton halo nuclei underneath and above coulomb barrier are still rare. Some elastic scattering experiments have additionally been accounted for ^{8}B on light mass target ^{12}C [20-22], ^{27}Al [23], intermediate mass target ^{58}Ni [1] and heavy mass target^{208}pb [24,4]. Theories of theoretical examinations of ^{8}B elastic scattering data with different nuclei at different energies have been performed in the most recent years. The greater part of this data is condensed in the survey articles by J. J. Kolata et al. [25].

It is notable that a good estimation of ^{8}B nucleus can be displayed as a core (^{7}Be) surrounded by one loosely bound valence proton. This supposition is bolstered by the fact that the valence proton is distributed in a spatial district which is much larger than the core. In this way, so as to supplement our examination, we embrace another estimate for ^{8}B as a core (^{7}B) and valence neutron. This configuration is proposed beforehand by J. Rangel et al. [26] to accomplish a comparative study of the break up effects on account of one-proton-halo and one-neutron-halo projectiles. Despite the fact that, its separation energy is extremely high, this configuration assumes no applicable role in the collision dynamics.

The main aim of the present investigation is to portray hypothetically the experimental angular dependences of the cross sections for the scattering of ^{8}B nucleus by ^{208}pb nucleus at 50 MeV (just at coulomb barrier) and 170.3 MeV [27]. The reaction cross sections are additionally considered. We studied the well-known Double Folding (DF) optical model potential to play out the present investigation.

Lukyanov et al. [28] contemplated the structure of ^{8}B utilizing Optical Model (OM) potential computations. They used DF optical model potential to calculate the elastic scattering cross section of ^{8}B on ^{12}C, ^{58}Ni and ^{208} Pb targets. The real part incorporates direct and exchange terms and the imaginary part contingent on high energy approximation method. They concluded that, their microscopic DF potential can be used well in analyzing reactions of systems include very exotic nuclei for example halo nucleus ^{8}B.

S. R. Mokhtar et al. [29] used semi phenomenological and microscopic DF potentials in the framework of OM potential to calculate the elastic scattering differential cross section of ^{8}B on ^{27}Al at incident energies above the coulomb barrier, namely 21.7 and 15.3 MeV. Four different shapes of ^{8}B density distribution are considered. Great concurrence with the experimental data is obtained without renormalization factors. They found that the

reliance of the angular distribution on ^{8}B density shape decrease when the incident energy increases.

Despite the fact that, phenomenological optical potentials are frequently used to depict the elastic scattering of heavy ions, the use of determined potentials is important because such potentials require information data either from other nuclear processes such as a nucleon-nucleon scattering or from nuclear models which should be checked firstly with these lines. Such calculations and computations enable one to anticipate the potentials for the systems for which elastic scattering data are not accessible. We have made a stride toward this path for the real part of the optical potential by using the DF model approximation, while the imaginary part is either parameterized by Woods-Saxon (WS) form or in the same form as real folded potentials and different strengths.

This paper is organized as follows: Sect.2 contains the depiction of the OM potential that we utilized, while the outcomes are introduced in Sec.3. At long last, our fundamental conclusions are exhibited in Sec.4.

2. ELASTIC SCATTERING ANALYSIS

In this article, we analysed the elastic scattering cross section of the system ^{8}B + ^{208}pb at two different energies; 50 and 170.3 MeV based on DIM3Y effective NN interaction association with the zero-range approximation by evaluating the real DF potential in the frame work of the OM. The concurrence of the resultants with the elastic scattering experimental data is our tool for the verification of the used model.

2.1 Optical Model Potential

The total OM potential represents the nuclear interaction between the two interacting nuclei in the form of three additive terms as

$$U(R) = V(R) + iW(R) + V_C(R), \quad (1)$$

where, V(R), W(R) and V_C (R) are real, imaginary parts and repulsive coulomb potentials, respectively. In the construction of the OM, the real part can be obtained by folding the effective nucleon – nucleon (NN) interaction with the nucleon densities in the incident and target nuclei. Thus, the resultant DF potential $V_{DF}(R)$ may be formulated as [30].

$$V_{DF}(R) = \iint \rho_1(r_1)\rho_2(r_2)\, V_{NN}(R + r_2 - r_1)dr_1 dr_2, \quad (2)$$

Where $\rho_1(r_1)$ and $\rho_2(r_2)$ are the nuclear matter density distributions for projectile (^{8}B) and target (^{208}pb) nuclei. R is the vector that separate between the projectile and the target centers of mass. Here, we take the NN interaction to be density independent form of M3Y effective interaction (*DIM3Y*) with a zero–range approximation in the form [30].

$$V_{NN}(s) = 7999\frac{e^{-4.0s}}{4.0s} - 2134\frac{e^{-2.5s}}{2.5s} - 276\left(1 - 0.005\frac{E}{A}\right)\delta(s), \quad MeV \quad (3)$$

$$s = \left|R + r_2 - r_1\right|.$$

E is the bombarding laboratory energy, A is the mass number of the projectile and S is the distance between two nucleons.

As a first step, the imaginary part is treated phenomenologically by considering the Woods-Saxon (WS) shape*:*

$$W(R) = W_I\left[1 + \exp\left(\frac{R - R_I}{a_I}\right)\right]^{-1}, \quad (4)$$

where W_I is the potential depth, a_I is the diffuseness. The radius R_I can determine by using the relation $R_I = r_I(A_P^{1/3} + A_T^{1/3})$ with a reduced radius r_I. *A_P and A_T* is the mass numbers of different projectiles and target respectively. Thus, for the nucleus-nucleus DF potential case, the nuclear potential takes the form

$$U_{P1}(R) = N_R V_{DF}(R) + iW(R) \quad (5)$$

As a second step, the imaginary part is replaced by the DF potential also; hence the nuclear potential takes one of the two forms:

$$U_{P2}(R) = V_{DF}(R) + iN_I V_{DF}(R) \quad (6)$$

And

$$U_{P3}(R) = (N_R + iN_I)V_{DF}(R), \quad (7)$$

where N_R and N_I are the real and imaginary renormalization factors.

2.2 Matter Density Distributions

Beside the effective NN interaction, nuclear matter density distributions for the colliding nuclei are required for the input to the folding calculation.

As for the projectile nucleus, considering that ^{8}B nucleus is composed of a (core + halo nucleon). Thus, we have two choices; (^{7}Be and one halo proton) and (^{7}B and one halo neutron). Consequently, the total density $\rho_2(r_2)$ of ^{8}B can be written in two forms:

$$\rho_{8_B}(r) = \rho_{7_{Be}}(r) + \rho_{P}(r), \tag{8}$$

and

$$\rho_{8_B}(r) = \rho_{7_B}(r) + \rho_{n}(r) \tag{9}$$

The cores densities $\rho_{7_{Be}}(r)$ and $\rho_{7_B}(r)$ are presented in Gaussian form, whilst, the neutron and proton halo density is taken to be harmonic oscillator (HO) density. So, according to equations (8,9):

$$\rho_{7_B,{}^{7}Be}(r) = \left(\frac{3}{2\pi\, R_C^2}\right)^{3/2} \exp\left(-\frac{3r^2}{2\, R_C^2}\right), \tag{10}$$

and

$$\rho_{P,n}(r) = \frac{5}{3}\left(\frac{5}{2\pi R_h^2}\right)^{3/2}\left(\frac{r}{R_h}\right)^2 \exp\left(-\frac{5r^2}{2R_h^2}\right). \tag{11}$$

where, C and h are denoted as core and nucleon halo. So, the root mean square radii (R_C , R_h) of those are related to the matter radius (R_m) of the ^{8}B as:

$$A_m R_m^2 = N_C R_C^2 + N_h R_h^2 \tag{12}$$

The symbols, *N* and A_m are number of nucleons in the core, halo (N_C, N_h) and ^{8}B, respectively. Hence, the total matter density distribution for ^{8}B is given by:

$$\rho_m(r) = N_C \rho_C(r) + N_h \rho_h(r) \tag{13}$$

The values of R_C, R_m are taken from [31], 2.31 and 2.38 fm, respectively, and this density produces R_h =2.82 fm.

However, in [32,33] authors are spotted light on a contraction of the core ^{7}Be inside ^{8}B due to the existence of loosely bound valence proton. As a result, the deduced core radius R_C = 2.24 fm is smaller than ^{7}Be matter radius R_m= 2.31 fm. Therefore, aiming to a successful description of the experimental data with our model, we recalculate the density distribution using R_C = 2.24 fm and R_m= 2.58 fm. For The other alternative of ^{8}B configuration showed in equation (9); R_m= 2.58 fm, ^{7}B (R_C = 2.42 fm) [34] and neutron halo (R_h = 3.49 fm).

Two- parameter Fermi (2PF) shape is considered for ^{208}pb density distribution, [35]:

$$\rho_{2PF}(r) = \rho_{\circ}\left[1 + \exp\left(\frac{r - 6.621}{0.551}\right)\right]^{-1}, \tag{14}$$

The parameter $\rho_{\circ}$ can be produced from the normalization condition $4\pi\int \rho(r) r^2 dr = A$, where A is the mass number.

3. RESULTS AND DISCUSSION

In the structure of Optical Model (OM), the elastic scattering cross section of the system ^{8}B + ^{208}pb is calculated using DF potential dependent on DIM3Y effective NN interaction association with the zero-range approximation. In our examination, we used three different models of Optical Model Potential (OMP), that we called U_{P1}, U_{P2} and U_{P3}, respectively. In the first approach, the real part is calculated microscopically, while, the imaginary part is calculated phenomenologically, as appeared in (6). In the other two approaches, the optical potential is a complex potential, where the real and imaginary parts have the same shape (7,8).

The derived potentials (2) are calculated using the folding code DFPOT [36], as a initial step. At that point, the angular distribution of the ^{208}pb (^{8}B,^{8}B) ^{208}pb elastic scattering at energies 50 and 170.3 MeV are analyzed in the framework of the Distorted –Wave Born approximation (DWBA) by means of the computer code HIOPTM-94 [37]. The DF potentials acquired by expressions (2) are fed into the code to represent the real part of the optical potential, while the imaginary part is considered phenomenologically by the WS form (4,5). It is found that successful reproduction of the data can be gotten by considering N_R =1. This potential is symbolized as (U_{P1}).

For a fit to a few data points of elastic scattering at the coulomb barrier or higher than the coulomb barrier, the number of adjustable parameters ought to be as little as conceivable on the grounds that there are noteworthy ambiguities for the derived potentials; the hidden issue is that the elastic scattering cross section is sensitive to the phase shifts and reflection coefficients. Consequently, in the subsequent advance, the imaginary WS part is supplanted likewise by DF potential; for this situation the free parameters are N_R and N_I. This implies both the real and imaginary parts of the folded potentials are assumed to have the same shape and different strengths. This potential is denoted as either (U_{P2}) or (U_{P3}) contingent upon the value of N_R (fixed or variable). For the system under study, we found that the experimental data well produced by considering N_R =1 and N_I is variable. Best fits are obtained by minimizing the χ^2 value, [30].

$$\chi^2 = \frac{1}{N_D}\sum_{i=1}^{N_D}\left[\frac{\sigma_{th}(\theta_i)-\sigma_{\exp}(\theta_i)}{\Delta\sigma_{\exp}(\theta_i)}\right]^2 , \qquad (15)$$

where $\sigma_{th}(\theta_i)$ and $\sigma_{\exp}(\theta_i)$ are the theoretical and experimental cross sections, respectively at angle (θ_i), $\Delta\sigma_{\exp}(\theta_i)$ is the experimental error, and N_D is the number of data points. An average value 10% is used for the experimental errors of all considered data.

Table 1. The best fitting optical potential parameters obtained using the folded potentials in three different models U_{P1}, U_{P2} and U_{P3} to analyze ^{208}pb (^{8}B,^{8}B) ^{208}pb elastic scattering at 50MeV. ^{8}B is treating as (^{7}Be+P) with matter radii R_m=2.38, 2.58 and R_m=2.58 as (^{7}B+n) within cases (a), (b) and (c) respectively

Model	N_R	N_I	W_I MeV	r_I fm	a_I fm	J_R MeV.fm^3	J_I MeV.fm^3	σ_R mb	χ^2
(a)									
U_{P1}	1	---	6.35	1.94	0.47	413.02	43.89	773.30	51.73
U_{P2}	1	4.75	----	----	----	413.02	1960.84	393.70	86.54
U_{P3}	1.9	4.75	----	----	----	784.74	1960.84	417.20	80.02
(b)									
U_{P1}	1	---	6.31	1.97	0.48	415.29	43.67	778.6	51.64
U_{P2}	1	4.18	----	----	----	415.29	1735.34	551.0	64.91
U_{P3}	2.47	0.43	----	----	----	1025.53	180.64	367.9	82.84
(c)									
U_{P1}	1	---	6.36	2.03	0.66	413.14	43.96	775.4	51.65
U_{P2}	1	4.75	----	----	----	413.10	1961.22	480.3	69.57
U_{P3}	2	4.75	----	----	----	826.21	1961.22	510.9	66.50

Table 2. The best fitting optical potential parameters obtained using the folded potentials in three different models U_{P1}, U_{P2} and U_{P3} to analyze ^{208}pb(^{8}B,^{8}B) ^{208}pb elastic scattering at 170.3 MeV. ^{8}B is treating as (^{7}Be+P) with matter radii R_m=2.38, 2.58 and R_m=2.58 as (^{7}B+n) within cases (a), (b) and (c) respectively

Model	N_R	N_I	W_I MeV	r_I fm	a_I fm	J_R MeV.fm^3	J_I MeV.fm^3	σ_R mb	χ^2
(a)									
U_{P1}	1	---	26.91	1.53	0.029	392.29	121.52	3247	1.87
U_{P2}	1	3.08	----	----	----	392.29	1210.08	3450	2.29
U_{P3}	1.51	0.50	----	----	----	592.46	196.14	2828	5.08
(b)									
U_{P1}	1	---	62.81	1.52	0.061	394.41	274.70	3137	1.88
U_{P2}	1	1.56	----	----	----	394.41	613.14	3452	3.12
U_{P3}	0.69	0.80	----	----	----	272.85	315.53	3135	3.29
(c)									
U_{P1}	1	---	34.04	1.53	0.02	392.60	152.58	3193	1.88
U_{P2}	1	2.09	----	----	----	392.30	818.18	3455	2.63
U_{P3}	0.87	0.90	----	----	----	341.35	353.07	3111	3.38

The results of $U_{P1,}$ U_{P2} and U_{P3} are appeared in Fig. (1a-1d) and Fig. (2a, 2b) for incident energies 50 and 170.3 MeV. The best fit parameters extracted from the auto search using the HIOPTM-94 code are recorded in the Tables (1,2). It is plainly seen that, U_{P1} gives good fitting at both incident energies and this is reflected on the chi square values shown in Tables. On the other hand, one can see that; a quite good fitting is accomplished for both energies by using U_{P2} than U_{P3}. The accomplishment of these potentials can also be resulted from the corresponding reaction cross section σ_R values listed in the Tables.

Recently, J.S. Wang et al. [38] measured the elastic scattering of ^{8}B on ^{208}pb at 170.3 MeV. The analyses of these data have been performed in terms of phenomenological OM using the WS potential and the corresponding σ_R =3342 mb. Besides, the determined σ_R using an OM calculation with a systematic single-folding potential is 3270 mb by the same group [26]. All around as of late, V. K. Lukyanov et al. [28]

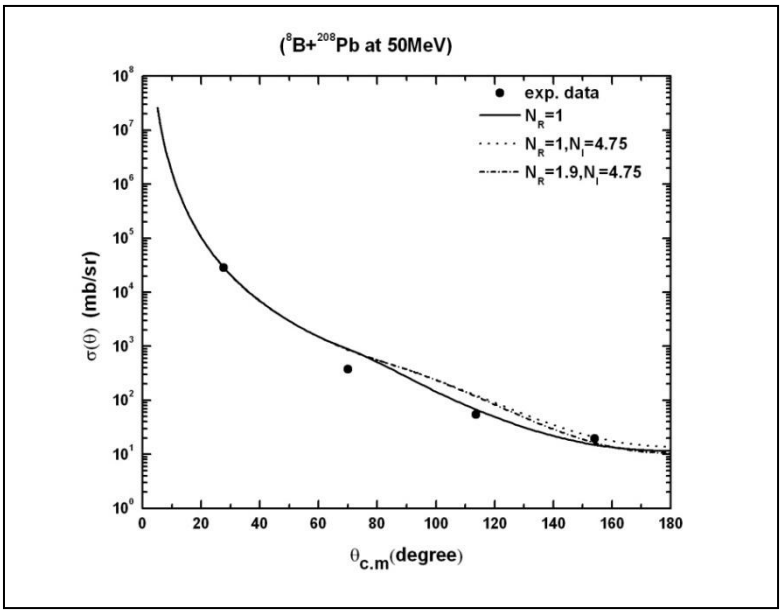

Fig. 1(a).

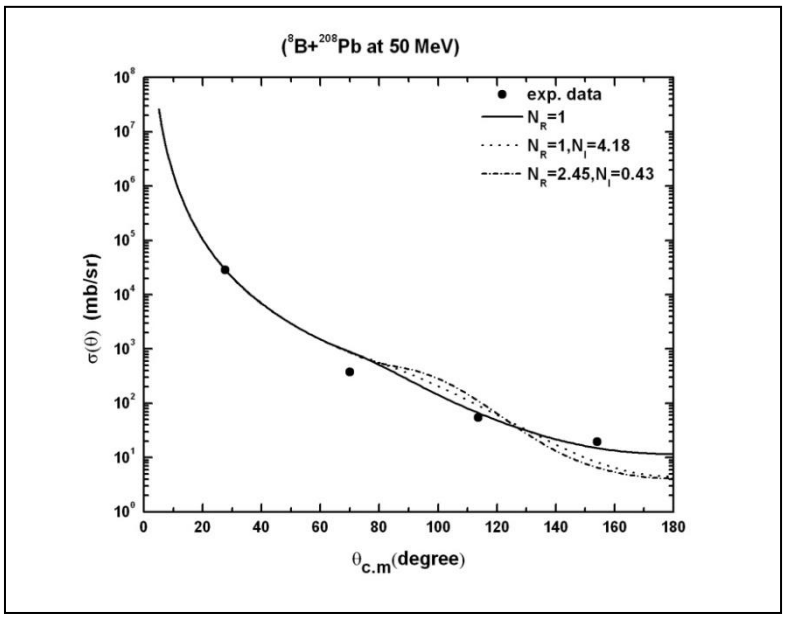

Fig. 1(b).

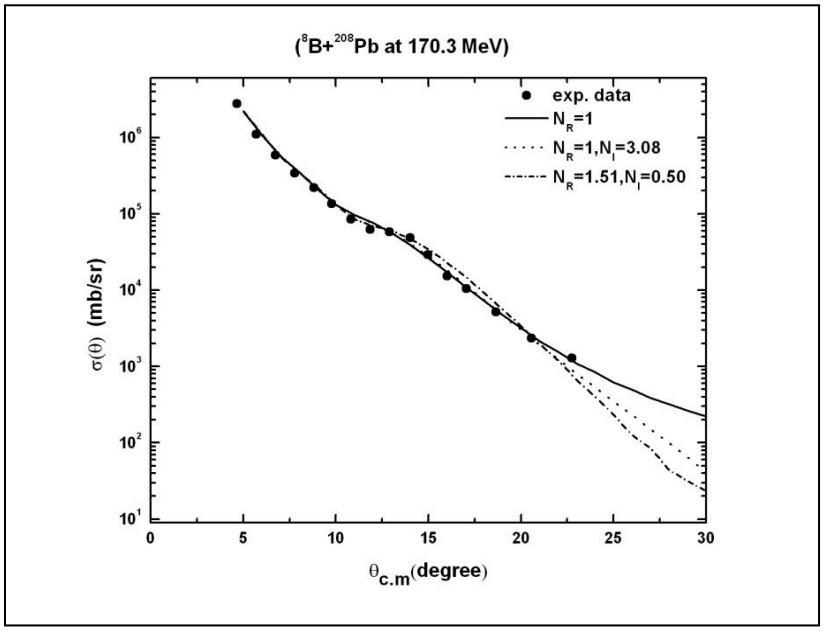

Fig. 1(c).

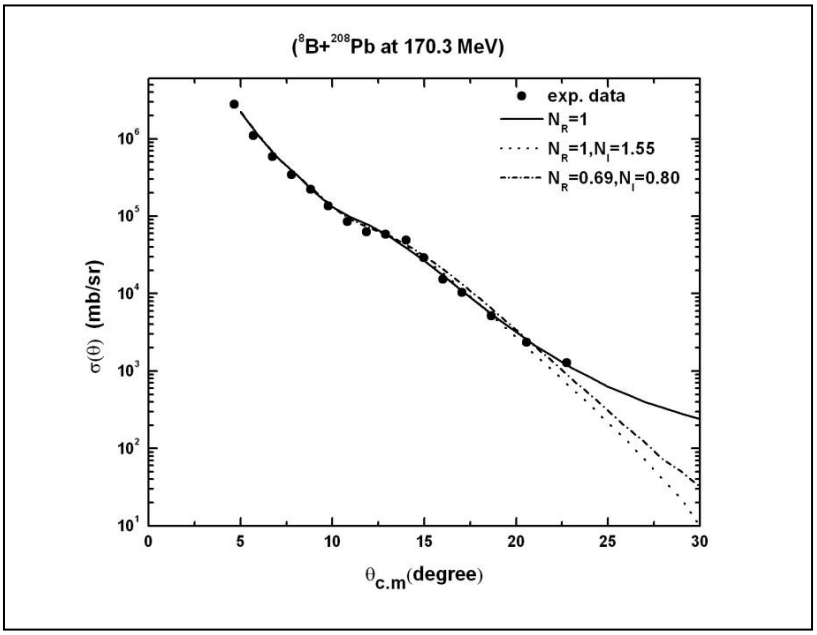

Fig. 1(d).

Fig. 1. The elastic scattering cross sections for ^{8}B+^{208}Pb obtained from optical model calculations employing DF potentials for treating ^{8}B nucleus as (^{7}Be+p) in comparison with the experimental data

calculated σ_R using two distinct densities of ^{8}B within density dependent DF formalism (CDM3Y6). They found that the acquired σ_R from three-cluster (3CM) and variational Monte Carlo model (VCM) densities calculations are 3226.73 mb, 3158.3 mb, respectively.

In the present examination, our calculations gave the estimations of σ_R which be reliable with the estimations of [24,28] for U_{P1}, while U_{P2} and U_{P3} give somewhat greater and smaller than [24,38] and [30] using VMC, respectively. In contrast, by using reduced (R) core radius, we

got σ_R of U_{P1} and U_{P3} less than [24,28,38]. A similar deviation is found by U_{P2}. However, it is tally with that written in [28] using 3CM of ^{8}B. This distinction might be ascribed to the choice of the model that we are used. Lamentably, no measured values of σ_R at coulomb barrier energy to be contrasted with calculated ones.

Additionally, the consequences of the two structures of ^{8}B (proton or neutron halo), similarly describe satisfactorily relevant experimental data. This coincides with the internal structure of the nucleus as there is no difference between two nucleons. Along these lines, this affirms the legitimacy of the halo structure of the ^{8}B nucleus within this model.

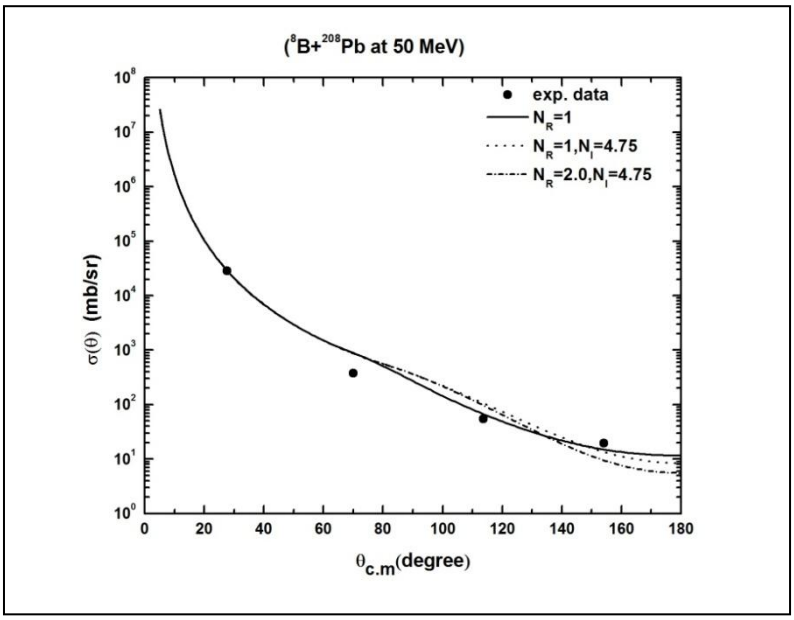

Fig. 2(a).

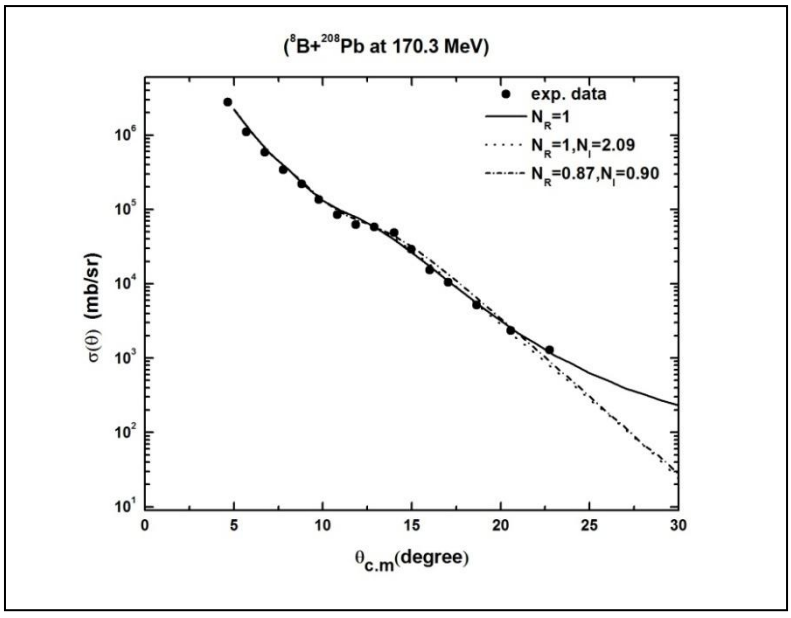

Fig. 2(b).

Fig. 2. The elastic scattering cross sections for ^{8}B+^{208}Pb obtained from optical model calculations employing DF potentials for treating ^{8}B nucleus as (^{7}B+ n) in comparison with the experimental data

4. CONCLUSION

We investigated the elastic scattering of the halo nucleus ^{8}B projectile by the heavy ^{208}pb target at 50 and 170.3 MeV at and far above the coulomb barrier in the framework of the OM using three different potentials;$U_{P1,}$ U_{P2} and U_{P3}. The potentials effectively recreate the experimental data. We found that U_{P1} gives the best portrayal of the elastic scattering data at the two energies. Our choice of the density distribution of ^{8}B with three imaginary parameters gives a good coherency between the hypothetical and experimental results.

Furthermore, the results of the two structures of ^{8}B (proton or neutron halo) of similarly describe satisfactorily relevant experimental data. This coincides with the internal structure of the nucleus as there is a strong nuclear force between proton and neutron inside the nucleus. Despite the fact that, neutron halo separation energy is extremely high, this configuration assumes no applicable role in the collision dynamics. Thus, this confirms the validity of the halo structure of the ^{8}B nucleus within this model. Therefore, it is worth concluding that considering the halo structure of ^{8}B is essential to obtain successful predictions of the elastic scattering data.

So the structure of halo nuclei to be a core and one or two valance nucleon regardless of whether it is a proton or a neutron allow for more structure and studies in the future.

These potentials produce σ_R either larger or smaller than that given using other OM potentials. This distinction could be credited to the selection of the model that we used. Unfortunately, no measured values of σ_R at coulomb barrier energy to be compared with calculated ones. Likewise, the lack of experimental data of this researched system below and above the barrier doesn't permit any positive ends to be drawn concerning the variation of the volume integral of the real and imaginary parts of the OMP as a function of incident energy.

COMPETING INTERESTS

Authors have declared that no competing interests exist.

REFERENCES

1. Aguilera EF, et al. Reaction cross sections for ^{8}B, ^{7}Be, and ^{6}Li+^{58}Ni near the Coulomb barrier: Proton-halo effects, Phys. Rev. 2009;C79:021601(R).
2. Aguilera EF, et al. Angular momentum limit for fusion of halo and weakly bound systems, Phys. Rev. 2012;C85:014603.
3. Pakou A, et al. Fusion cross sections of ^{8}B+^{28}Si at near-barrier energies, Phys. Rev. 2013;C87:014619.
4. Yang YY, et al. Elastic scattering of the proton drip-line nucleus ^{8}B off a ^{nat}Pb target at 170.3 MeV. Phys. Rev. 2013; C87:044613.
5. Tanihata I, et al. Measurement of interaction cross sections using isotope beams of Be and B and isospin dependence of the nuclear radii. Phys. Lett. 1988;B206:592.
6. Obuti MM, et al. Interaction cross section and interaction radius of the ^{8}B nucleus. Nucl. Phys. 1996;A609:74.
7. Wang J, et al. RMF calculation and phenomenological formulas for the rms radii of light nuclei. Nucl. Phys. 2001; A691:618.
8. Kelley JH, et al. Study of the Breakup Reaction ^{8}B--> ^{7}Be+ p: Absorption Effects and E-2 Strength. Phys. Rev. Lett. 1996; 77:5020.
9. Jin SL, et al. Reaction mechanism of ^{8}B breakup at the Fermi energy. Phys. Rev. 2015;C91, 054617.
10. Warner RE, et al. Elastic scattering of 10 MeV ^{6}He from ^{12}C, ^{nat}Ni, and ^{197}Au. Phys. Rev. 1995;C51:178.
11. Terakopian GM, et al. Two-neutron exchange observed in the ^{6}He+^{4}He reaction. Phys. Lett. 1998;B426:251.
12. Benjamim EA, et al. Elastic scattering and total reaction cross section for the ^{6}He+ ^{27}Al system. Phys. Lett. 2007;B647:30.
13. Acosta L, et al. Elastic scattering and α-particle production in ^{6}He + ^{208}Pb collisions at 22 MeV. Phys. Rev. 2011;C84:044604.
14. Kakuee OR, et al. Long range absorption in the scattering of ^{6}He on ^{208}Pb and ^{197}Au at 27 MeV, Nucl. Phys. 2006;A765:294.
15. Rusek K, et al. Dipole polarizability of ^{6}He and its effect on elastic scattering. Phys. Rev. 2003;C67:041604(R).
16. Kakuee OR, et al. Elastic scattering of the halo nucleus ^{6}He from ^{208}Pb above the Coulomb barrier. Nucl. Phys. 2003;A728 : 339.

17. Sanchez-Benıtez AM, et al. Study of the elastic scattering of ^{6}He on ^{208}Pb at energies around the Coulomb barrier. Nucl. Phys. 2008;A803:30.
18. Johnson RC, et al. Elastic scattering of halo nuclei. Phys. Rev. Lett. 1997;79:2771.
19. Di Pietro A, et al. Elastic Scattering and Reaction Mechanisms of the Halo Nucleus ^{11}Be around the Coulomb Barrier. Phys. Rev. Lett. 2010;105:022701.
20. Pecina I, et al. Quasielastic scattering of ^{8}B and ^{7}Be on ^{12}C at 40 MeV/nucleon. Phys. Rev. 1995;C52:19.
21. Tabacaru G, et al. Scattering of ^{7}Be and ^{8}B and the astrophysical ^{17}S factor, Phys. Rev. 2006;C73:025808.
22. Barioni A, et al. Elastic scattering and total reaction cross sections for the ^{8}B, ^{7}Be, and ^{6}Li+ ^{12}C systems. Phys. Rev. 2011;C84: 014603.
23. Morcelle V, et al. ^{8}B+ ^{27}Al scattering at low energies. Phys. Rev. 2017;C95:014615.
24. La Commara M, et al. ^{8}B+ ^{208}Pb Elastic Scattering at Coulomb Barrier Energies. EPJ Web of Conferences. 2017;163: 00032.
25. Kolata JJ, et al. Elastic scattering, fusion, and breakup of light exotic nuclei. Eur. Phys. J. 2016;A52:123.
26. Rangel J, et al. Effect of Coulomb breakup on the elastic cross section of the ^{8}B proton-halo projectile on a heavy, ^{208}Pb target, Phys. Rev. 2016;C93:054610.
27. El-Azab Farid M, Satchler GR. A density-dependent interaction in the folding model for heavy-ion potentials. Nucl. Phys. 1985;A438:525.
28. Lukyanov VK, et al. Probing the exotic structure of ^{8}B by its elastic scattering and breakup reaction on nuclear targets. Eur. Phys. J. 2017;A53:31.
29. Mokhtar SR, et al. Optical Model Analysis of ^{8}B+^{27}Al Elastic Scattering Above the Coulomb Barrier. J. Rad. Nucl. Appl. 2018; 3(1):1.
30. Satchler GR, Love WG. Folding model potentials from realistic interactions for heavy-ion scattering. Phys. Rep. 1979;55: 183.
31. Tanihata I, et al. Measurement of interaction cross sections using isotope beams of Be and B and isospin dependence of the nuclear radii. Phys. Lett. 1988;B206:592.
32. Nakada H, et al. E2 properties of nuclei far from stability and the proton-halo problem of ^{8}B", Phys. Rev. 1994;C49:886.
33. Vorobyov A, et al. An Ionization Spectrometer For Recoil Nuclei In Research On Elastic Small Angle Scattering Of Hadrons Instrum. Exp. Tech. 1982;24:1127.
34. Tel E, et al. Calculation of radii and density of $^{7-19}$B isotopes using effective Skyrme force. Commun. Theor. Phys. 2008;49(3): 696.
35. De Vries H, et al. Nuclear charge-density-distribution parameters from elastic electron scattering, Atom. Data Nucl. Data Tables. 1987;36:495536.
36. Cook J. DFPOT - A program for the calculation of double folded potentials. Comput. Phys. 1982;25:125.
37. Clarke NM. Unpublished; 1994.
38. Wang JS, et al. ^{7}Be, ^{8}B+ ^{208}Pb Elastic Scattering at Above-Barrier Energies. J. Phys: Conf. Ser. 2013;420:012075.

Peer-review history:
The peer review history for this paper can be accessed here:
http://www.sdiarticle4.com/review-history/53312